REVIEW PAPER

Synthesis of metal-organic frameworks: A mini review

Yu-Ri Lee, Jun Kim, and Wha-Seung Ahn[†]

Department of Chemistry and Chemical Engineering, Inha University, Incheon 402-751, Korea
(*Received 10 May 2013 • accepted 30 July 2013*)

Abstract−Metal organic frameworks (MOFs) are porous crystalline materials of one-, two-, or three-dimensional networks constructed from metal ions/clusters and multidentate organic linkers via coordination bonding, which are emerging as an important group of materials for energy storage, CO_2 adsorption, alkane/alkene separation, and catalysis. To introduce newcomers in chemical engineering discipline to the rapidly expanding MOF research works, this review presents a brief introduction to the currently available MOFs synthesis methods. Starting from the conventional solvothermal/hydrothermal synthesis, microwave-assisted, sonochemical, electrochemical, mechanochemical, ionothermal, dry-gel conversion, and microfluidic synthesis methods will be presented. Examples will be limited to those representative MOF structures that can be synthesized using common organic ligands of 1,4-benzenedicarboxylic acid (and its functionalized forms) and 1,3,5-benzenetricarboxylic acid, in conjunction with metal nodes of Zn^{2+}, Cu^{2+}, Cr^{3+}, Al^{3+}, Fe^{3+} and Zr^{4+}. Synthesis of widely-investigated zeolitic imidazolate framework (ZIF) structure, ZIF-8 is also included.

Key words: Metal Organic Frameworks (MOFs), Zeolitic Imidazolate Frameworks (ZIFs), Solvothermal/Hydrothermal Synthesis, Microwave, Sonochemistry, Electrochemical Synthesis, Mechanochemical Synthesis

INTRODUCTION

Metal organic frameworks (MOFs) are a class of crystalline organic-inorganic hybrid compounds formed by coordination of metal clusters or ions with organic linkers, in which bivalent or trivalent aromatic carboxylic acids or N-containing aromatics are commonly used to form frameworks with zinc, copper, chromium, aluminum, zirconium, and other elements [1-9]. Since MOFs have high surface areas and high pore volumes in uniformly sized pores as well as high metal content, they have emerged as interesting materials for various applications in energy storage [10,11], CO_2 adsorption [12,13], hydrocarbon adsorption/separation [14-16], catalysis [17-19], sensor [20], magnetism [21], drug delivery [22], luminescence [23,24], and others. Recent extensive review articles on MOFs have dealt with synthesis, characterization, surface modification, and applications [3-5,19,25,26]. Our aim is to provide more specific and engineering-orientated information on the synthesis of MOF materials expected for use as adsorbents and catalysts in industry. For more broad understanding on the topic, the review article by Stock and Biswas [26] is strongly recommended.

Thus far, MOFs have been generally prepared via hydrothermal or solvothermal synthesis routines by electrical heating in small scales, which take reaction time from several hours to days. Efforts were primarily given to preparing high quality single crystals adequate for structural analysis in dilute liquid phase conditions. Alternative synthesis methods were attempted afterward in an effort to shorten the synthesis time and to produce smaller and uniform crystals, such as microwave-assisted [16,27,28], sonochemical [29-31], electrochemical [32,33], and mechanochemical methods [34,35]. Limited synthesis scale-up for industrial applications was also conducted

[36,37]; sometimes, detailed investigations on the optimization of MOF synthesis conditions in these studies were carried out in order to obtain high yields of solid products for industrial applications.

In this mini review, we examine MOF synthesis methods reported in the open literatures. Attention is only given to the preparation of the MOF structures described in Scheme 1, which are prepared using an organic ligand such as H_2BDC (1,4-benzenedicarboxylic acid) and its functionalized form (H_2BDC-NH_2; 2-amino-1,4-benzenedicarboxylic acid, H_2BDC-$(OH)_2$; 2,5-dihydroxy-1,4-benzenedicarboxylic acid), or H_3BTC (1,3,5-benzenetricarboxylic acid). MOF-5 reported in 1999 in Nature by Yagi et al. had attracted huge attention due to its robust open framework structure supporting permanent porosity and simple design strategy for pore size control [38], which ignited active investigations toward MOF applications to gas storage [39] and heterogeneous catalysis [40]. However, after its weak hydrothermal stability was revealed, attention shifted to HKUST-1 [41] because of its good stability against moisture, excellent thermal stability, and relatively easy synthesis. Currently, MIL-101 seems to be the most frequently adopted material for catalysis and adsorption. MIL-101($Cr_3O(F/OH)(H_2O)_2[C_6H_4(CO_2)_2]_3$) by Ferey et al. is a robust MOF with high surface area, typically prepared hydrothermally using a chromium salt and H_2BDC in an autoclave under autogenous pressure conditions [42]. MIL-101 is unique in that it exhibits exceptional stability against moisture and other chemicals, and is composed of coordinatively unsaturated Cr-sites in high concentration available for catalysis and adsorption [43-45]. MIL-101 with a BET (Brunauer, Emmett, and Teller) surface area greater than 4,000 m^2/g is, however, very difficult to obtain because the impurities produced by the unreacted H_2BDC or recrystallized H_2BDC are present both outside and within the pores of MIL-101 [46]. NH_2-functionalization in MOF-5 produces IRMOF-3, which imparts basicity to MOF-5 framework and produces an enhancement in CO_2 capture capacity [39], provides catalytic sites for Knoevenagel condensa-

[†]To whom correspondence should be addressed.
E-mail: whasahn@inha.ac.kr
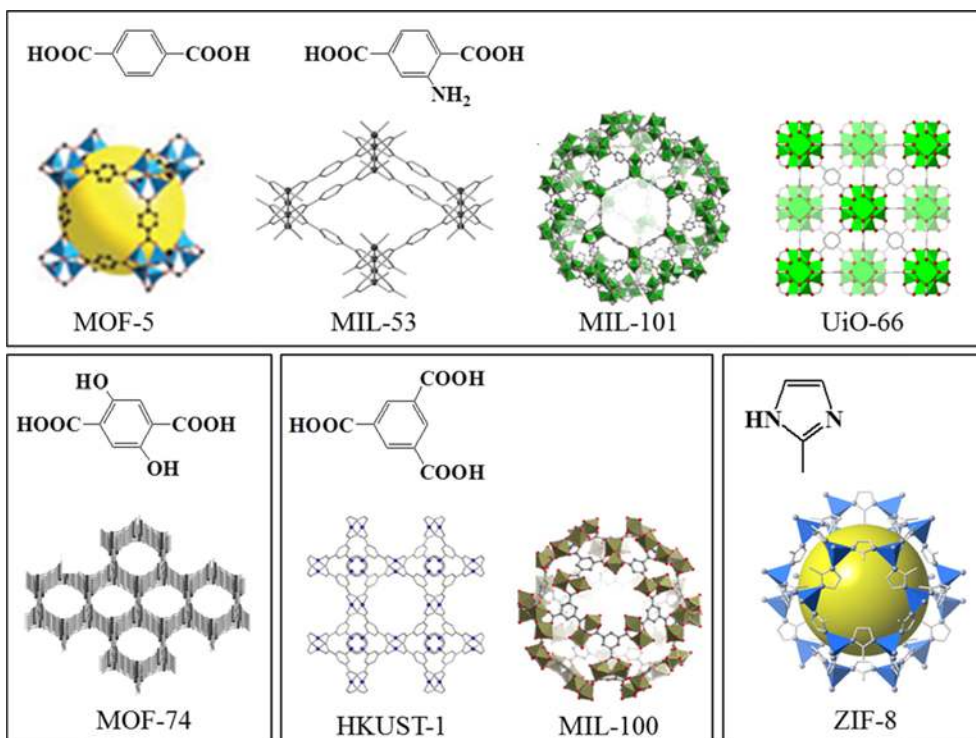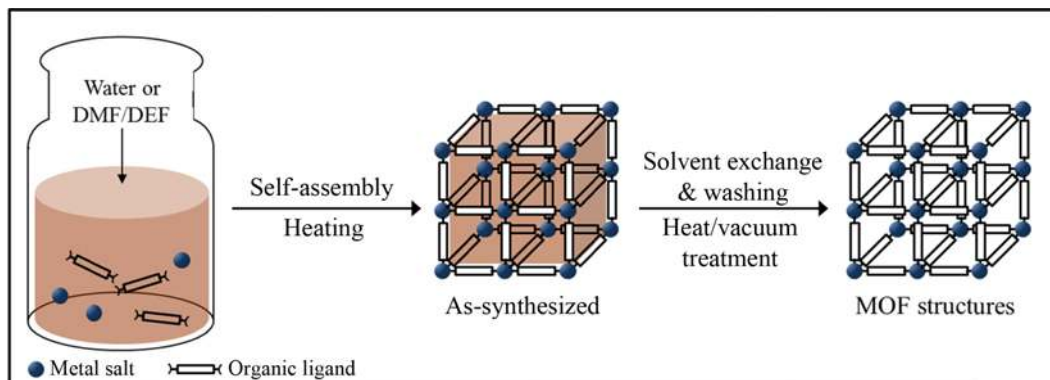
Scheme 1. Representative MOF structures.

tion reaction [47], and acts as diverse post-synthesis organic functionalization sites for transition metal complex binding [17]. MOF-74 has attracted interest due to its high CO_2 adsorption capacity under practical atmospheric pressure conditions [13,28,48,49], MIL-53 due to unique pore expansion/contraction behavior upon interaction with guest molecules [50-52] in gas storage and separation, and MIL-100 due to its high stability and high catalytic activity for Friedel-Crafts benzylation [53] also deserve mentioning. UiO-66 is a Zr(IV)-based MOF having exceptional hydrothermal stability and is a model compound for diverse post-synthesis organic functionalization [54].

Zeolitic imidazolate frameworks (ZIFs) are a family of microporous materials in which Zn or Co atoms are linked through N atoms of ditopic imidazolates to form a range of neutral framework structures [55,56]. The frameworks of ZIF compounds can be represented by $T(Im)_2$ (Im=imidazolate and its derivative, T=tetrahedrally coor-

dinated metal ion) similar to the $(Al)SiO_2$ frameworks of (alumino) silicate zeolites; in particular the T-Im-T angle of 145° is close to the Si-O-Si angle typically found in zeolites [56]. ZIFs materials can have structures analogous to the standard zeolite topology such as *rho*, *sod*, *gme*, *lta*, and *ana*. Among the ZIFs, ZIF-8 is the most widely-investigated structure due to its high thermal and chemical stability [56], and is also included in this review for its preparation. The synthesis methods employed for these MOF structures and their key findings are listed in Table 1 [13,16,27-29,31,32,39,41,42,45,52,53,56-67].

CONVENTIONAL SOLVOTHERMAL SYNTHESIS (SCHEME 2)

MOFs have been synthesized solvothermally via conventional electric heating in small scale in vials or sealed NMR tubes, and

Scheme 2. Conventional solvothermal synthesis of MOF structures.

Table 1. Representative MOF synthesis studies

Synthesis method[a]	Sample	Metal	Ligand[b]	Solvent[c]	Synthesis conditions — Conditions	Comments	Ref
CS	MOF-5	$Zn(NO_3)_2 \cdot 4H_2O$	H_2BDC	DMF/chlorobenzene	120 °C, 24 h	Isoreticular MOF (IRMOF-n) synthesis, methane storage (25 °C, 40 bar).	57
	UiO-66	$ZrCl_4$	H_2BDC	DMF	120 °C, 24 h	H_2 (−196 °C, 1 bar) and CO_2 (0 °C, 1 bar) adsorption.	58
	Cr-MIL-101	$Cr(NO_3)_3 \cdot 9H_2O$	H_2BDC	H_2O (add 1 M HF aq.)	220 °C, 8 h	Structure analysis.	42
	IRMOF-3	$Zn(NO_3)_2 \cdot 4H_2O$	$H_2BDC\text{-}NH_2$	DEF	85 °C, 96 h	CO_2 adsorption (25 °C, 1-40 bar).	39
	Al-MIL-53-NH_2	$Al(NO_3)_3 \cdot 9H_2O$	$H_2BDC\text{-}NH_2$	DMF	130 °C, 5 days	CO_2 pressure swing adsorption (50 °C, 5-20 bar).	52
	HKUST-1	$Cu(NO_3)_2 \cdot 3H_2O$	H_3BTC	H_2O/EtOH	180 °C, 12 h	Structure analysis.	41
	Fe-MIL-100	Metallic iron (Fe^0)	H_3BTC	H_2O (add HF+HNO_3, aq.)	150 °C, 6 days (pH<1)	Friedel-Crafts benzylation.	53
	ZIF-8	$Zn(NO_3)_2 \cdot 4H_2O$	HMeIm	DMF	85 °C, 72 h	High-throughput synthesis.	56
MW	MOF-5	$Zn(NO_3)_2 \cdot 4H_2O$	H_2BDC	NMP	800 W, 105 °C, 30 min	CO_2 adsorption (25 °C, 1-40 bar).	27
	Cr-MIL-101	$Cr(NO_2)_3 \cdot 9H_2O$	H_2BDC	H_2O/EtOH	600 W, 210 °C, 40 min	Benzene sorption (30 °C, 1 bar).	16
	Fe-MIL-53	$FeCl_3 \cdot 6H_2O$	H_2BDC	DMF	300 W, 150 °C, 10 min	Synthesis study.	45
	Fe-MIL-101-NH_2	$FeCl_3 \cdot 6H_2O$	$H_2BDC\text{-}NH_2$	DMF	150 °C, 15 min	Br-BODIPY[e] sorption (room temperature, 2 days).	59
	IRMOF-3	$Zn(NO_3)_2 \cdot 6H_2O$	$H_2BDC\text{-}NH_2$	DEF/EtOH	150 W, 35 s	Synthesis study.	60
	Co-MOF-74	$Co(NO_3)_2 \cdot 6H_2O$	H_4DHBDC	DMF : EtOH : H_2O=1:1:1	180 W, 130 °C, 60 min	CO_2 and H_2O adsorption (25 °C, 1 bar), CO_2 cycloaddition reaction.	28
	HKUST-1	$Cu(NO_3)_2 \cdot 3H_2O$	H_3BTC	EtOH	300 W, 140 °C, 1 h	Synthesis study.	61
	Cr-MIL-100	$C_3H_3CrO_9S_3$	H_3BTC	H_2O (HF aq. addition)	220 °C, 4 h	Synthesis study.	62
	ZIF-8	$Zn(NO_3)_2 \cdot 6H_2O$	HMeIm	DMF	140 °C, 3 h	Synthesis study.	63
SC	MOF-5	$Zn(NO_3)_2 \cdot 6H_2O$	H_2BDC	NMP	60 W, 30 min	CO_2 adsorption (25 °C, 1-40 bar).	29
	Mg-MOF-74	$Mg(NO_3) \cdot 6H_2O$	H_4DHBDC	DMF : EtOH : H_2O=15:1:1 (add TEA)	500 W, 1 h	CO_2 and H_2O adsorption (25 °C, 1 bar), CO_2 cycloaddition reaction.	13
	HKUST-1	$Cu(OAc)_2 \cdot 2H_2O$	H_3BTC	DMF : EtOH : H_2O=3:1:2 (add TEA)	150 W, 1 h	Synthesis study.	64
	PCN-6, PCN-6'	$Zn(NO_3)_2 \cdot 4H_2O$	H_3BPDC	DEF	PCN-6;300 W, 1h; PCN-6';150 W, 1 h	Interpenetration controlled MOF synthesis, CO_2 adsorption (25 °C, 1-30 bar).	31
EC	ZIF-8	$Zn(NO_3)_2 \cdot 6H_2O$	HMeIm	DMF (add TEA+NaOH aq.)	300 W, 1 h	Scale-up synthesis study, Knoevenagel condensation reaction.	37
	Al-MIL-53	$Al(NO_3)_3 \cdot 9H_2O$	H_2BDC	H_2O : DMF=90:10	Electrolyte : KCl, 90 °C, 10 mA	CO_2 adsorption (25 °C, 30 bar)	65
	Al-MIL-53-NH_2	$Al(NO_3)_3 \cdot 9H_2O$	$H_2BDC\text{-}NH_2$	H_2O : DMF=90:10	Electrolyte : KCl, 90 °C, 10 mA	Synthesis study, CO_2 adsorption (25 °C, 30 bar)	65
	HKUST-1	Copper plate	H_3BTC	MeOH	12-19 V, 1.3 A, 150 min	THT[f] removal (25 °C, 1 bar), H_2 storage (−196 °C, 40 bar), Kr/Xe separation (55 °C, 40 bar)	32
	Al-MIL-100	$Al(NO_3)_3 \cdot 9H_2O$	H_3BTC	H_2O/EtOH=25:75	Electrolyte : KCl, 60 °C, 50 mA	Synthesis study.	65
	ZIF-8	$Zn(NO_3)_2 \cdot 6H_2O$	HMeIm	DMF	Electrolyte : MTBS,[d] 25 °C, 50 mA	Synthesis study.	65
MC	HKUST-1	ZnO	H_3BTC	No solvent/MeOH	25 Hz, 15 min	Liquid-assisted grinding.	66
	ZIF-8	ZnO	HMeIm	DMF	5-60 min, 30 Hz	Synthesis study.	67
	ZIF-4	ZnO	HIm	DMF	5-60 min, 30 Hz	Synthesis study.	67

[a]CS=conventional solvothermal heating, MW=microwave-assisted, SC=sonochemical, EC=electrochemical, MC=mechanochemical synthesis

[b]H_2BDC=1,4-benzenedicarboxylic acid, $H_2BDC\text{-}NH_2$=2-amino-1,4-benzenedicarboxylic acid, H_3BTC=1,3,5-benzenetricarboxylic acid, HMeIm=2methyl imidazole, H_4DHBDC=2,5-dihydroxy-1,4-benzenedicarboxylic acid, H_3BPDC=4,4'-biphenyldicarboxylic acid, HIm=imidazole

[c]DMF=N,N-dimethylformamide, DEF=N,N-diethylformamide, NMP=N-methyl-2-pyrrolidone, HF=hydrofluoric acid, MeOH=methanol, EtOH=ethanol, TEA=triethylamine

[d]MTBS=tributylmethylammonium methyl sulfate

[e]Br-BODIPY=1,3,5,7-tetramethyl-4,4-difluoro-8-bromomethyl-4-bora-3a,4a-diaza-s-indacene (optical imaging contrast agent)

[f]THT=tetrahydrothiophene (sulfur odorant components)

high-throughput solvothermal syntheses are a powerful tool to accelerate the discovery of new MOF structures and to optimize synthesis protocols [56,68].

MOF-5 consists of octahedral Zn_4O clusters linked by ditopic linear BDC with a chemical formula of $Zn_4O·(BDC)_3·$guest molecules using a diffusion synthesis method [38] at low yield. Diffusion of triethylamine into a solution of zinc nitrate and H_2BDC in DMF/chlorobenzene resulted in the deprotonation of H_2BDC and reaction with Zn^{2+} ions. It is now replaced with a high-yield solvothermal method: an DEF (N,N-diethylformamide) solution mixture of $Zn(NO_3)_2·4H_2O$ and the H_2BDC are heated at 105 °C in a closed vessel to give crystalline MOF-5 [57]. IRMOF-3 is a member of the isoreticular MOF structures, in which Zn_4O clusters are linked by $BDC-NH_2$. The geometry for IRMOF-3 shows that the benzene ring lies in-plane with the Zn_4O ring and this configuration is stabilized by an intramolecular hydrogen bonding between the aromatic amino hydrogen atom and a carboxylate oxygen atom [69]. IRMOF-3 can be synthesized similarly under a given solvothermal condition: the substrate mixture of $Zn(NO_3)_2·6H_2O$ and $H_2BDC-NH_2$ is dissolved in DMF (N,N-dimethylformamide) or DEF, and the reaction mixture is heated in an oven at 90 °C for 24 h [47]. Room temperature high yield synthesis of MOF-5 (and MOF-74, MOF-177, HKUST-1) was also reported [70]: (1) H_2BDC (5.065 g) and triethylamine (TEA, 8.5 mL) were dissolved in 400 mL DMF, (2) $Zn(OAc)_2·2H_2O$ (16.99 g) was dissolved in 500 mL DMF, and (3) the zinc salt solution was added to the organic solution with stirring over 15 min, forming a precipitate, and the mixture was stirred for 2.5 h.

Although Zn(II)-based MOFs have many favorable attributes, their weak stability against moisture and protic solvents is likely to limit their industrial uses. This prompted efforts to develop more stable, chemically-resistant frameworks. Porous chromium-benzenedicarboxylate (so-called MIL-101, MIL stands for Material of Institute Lavoisier) has been investigated by Férey and co-workers [42]. MIL-101 is typically prepared hydrothermally using a chromium salt and H_2BDC with an aid of small amount of HF in an autoclave at 220 °C under autogenous pressure conditions for 8 h. MIL-101 is a robust MOF with a surface area greater than 4,000 m^2/g that consists of uniform mesopores (2.9 and 3.4 nm) accessible through two types of microporous windows (1.2 and 1.6×1.45 nm) and co-ordinatively unsaturated Cr-sites in high concentration available for adsorption and catalysis [42]. Many attempts have been made to increase the purity of the MIL-101 product by (1) rigorous three-step purification consisting of double filtration over two different filters, solvent treatments using hot ethanol and water, and finally fluoride-anion exchange using aqueous NH_4F solutions [71], (2) temperature-programmed synthesis to induce the formation of large residual carboxylic acid impurity crystals that can be isolated more easily [72], and (3) the addition of tetramethyl ammonium hydroxide to promote the dissolution of H_2BDC [73]. However, most reports of MIL-101 revealed BET surface areas of approximately 2,800-3,400 m^2/g, even after vigorous purification steps. The formation of impurity phases also resulted in low product-yields (ca. 42%) [74]. Therefore, it would be highly useful if an alternative synthesis method with simplified purification step was devised for MIL-101 in the near future.

Fe-MIL-100 is an iron(III) carboxylate with a large surface area, and obtained as a polycrystalline powder from a reaction mixture of 1.0 Fe^0 : 0.66 H_3BTC : 2.0 HF : .2HNO_3 : 280 H_2O that was kept at 150 °C in a Teflon-lined autoclave for 6 days, in which the pH remained acidic (<1) throughout the synthesis. The light-orange solid product was recovered by filtration and washed with deionized water. A treatment in hot deionized water (80 °C) for 3 h was applied to reduce the amount of residual H_3BTC (typically, 1 g of Fe-MIL-100 in 350 mL of water) followed by drying at room temperature [53].

MIL-53 is comprised of chains of corner-sharing $MO_4(OH)_2$ octahedra ($M=Cr^{3+}$, Al^{3+}) interconnected by BDC containing 1-D diamond-shaped tunnels [50,75]. MIL-53-NH_2 is an isoreticular structure with MIL-53, and linked by $H_2BDC-NH_2$. Both of the aluminum-containing MIL-53s structures, Al-MIL-53 and Al-MIL-53-NH_2, were reported to exhibit unusual CO_2 adsorption behavior, which was attributed to a "breathing" mechanism of the framework; the structure interchanges between the two large-pore (lp) and narrow-pore (np) forms, which have the same chemical composition and only differ in their pore width [76]. Recently, high-quality Al-MIL-53 and Al-MIL-53-NH_2 synthesis routes were reported: For Al-MIL-53, $AlCl_3·H_2O$ and H_2BDC were introduced to mixed solvent of DEF and EtOH, and the substrate mixture was heated at 110 °C for two days, whereas for Al-MIL-53-NH_2, $Al(NO_3)_3·9H_2O$ and $H_2BDC-NH_2$ were introduced to DMF, the substrate mixture was heated at 130 °C for five days [52].

Zirconium is highly resistant to corrosion and has a high affinity for hard oxygen donor ligands. A Zr(IV)-based MOF, UiO-66 (UiO= University of Oslo) has octahedral (~11 Å) and tetrahedral cages (~8 Å) connected by triangular windows (~6 Å) [54], and synthesized in powder form using $ZrCl_4$ and H_2BDC reacted in DMF at 120 °C for 24 h [58]. As anticipated from the strong Zr(IV)-carboxylate bonding, UiO-66 shows high chemical and thermal stability. UiO-66 is stable in polar protic solvents including water and alcohols. The crystallinity of UiO-66 was found to be retained even after treatment with aqueous HCl (pH=1) or aqueous NaOH (pH= 14) [54,77].

HKUST-1, first reported by Chui et al. [41], is one of the most well characterized and widely studied MOF materials. Cu_2-clusters in HKUST-1 are coordinated via carboxylate groups to form a so-called paddle-wheel unit in a three-dimensional porous cubic network [78]. The water or solvent molecules weakly coordinate with the Cu^{2+} sites and can be removed using mild activation in a vacuum, which leaves the framework with unsaturated open metal sites [79]. The main channels are square cross sections with diameters of ca. 0.9 nm, and the tetrahedral side consists of pockets with ca. 0.5 nm diameters connected to the main channels via triangular windows of approximately 0.35 nm in diameter [78,80]. HKUST-1 has been synthesized in various synthesis conditions because of its easy production, and reviewed in detail for its synthesis and applications by Kim et al. [81]. Recently, HKUST-1 was synthesized in a 1 liter Pyrex reactor, and optimization of synthesis conditions was investigated [36]. In a typical synthesis, 17.5 g of copper (II) nitrate hydrate (Sigma-Aldrich, 98%) and 8.4 g of H_3BTC (Sigma-Aldrich, 95%) were dissolved in 500 mL of ethanol (entry 1 in Table 2). H_3BTC concentration was 0.101 M and the mole ratio of Cu salt to ligand was kept at 9 : 5 in ethanol. The substrate mixture was then heated under reflux for 24 h with constant mechanical stirring at 300 rpm. Upon completion of the solvothermal reaction, the product was collected by filtration, and washed with deionized water and again with

Table 2. Textural properties and yield of HKUST-1 samples produced under different synthesis conditions[a] [36]

Entry	H_3BTC (M)	Synthesis time (h)	Stirring (RPM)	S_{BET} (m^2/g)[b]	V_{pore} (cm^3/g)[c]	Yield (%)
1	0.101	12	150	1854	0.78	21
2	0.101	24	150	1893	0.78	26
3	0.101	48	150	1877	0.78	22
4	0.101	72	150	1873	0.78	20
5	0.505	24	150	1395	0.62	34
6	0.808	24	150	1282	0.51	61
7	1.010	24	150	1250	0.47	74
8	1.010	24	200	1481	0.60	61
9	1.010	24	300	1737	0.72	40
10	1.515	24	150	1049	0.43	79

[a]Amount of copper salt was adjusted to keep the metal/ligand molar ratio to 9 : 5

[b]S_{BET}=specific surface area calculated by the BET method

[c]V_{pore}=total pore volume

ethanol. The powder product was dried at 373 K for 5 h in a vacuum oven. The BET surface areas of the samples after 12 to 72 h reaction remained almost constant. However, 24 h reflux conditions produced somewhat higher yield and the crystals steadily grew as the synthesis time increased in the size range of 1.5 to 3.5 μm. Product yield in 24 h synthesis increased significantly from 26 to 79% as the H_3BTC concentration was increased from 0.101 to 1.515 M (entry 2, 5, 7, and 10 in Table 2), but the BET surface area decreased from 1,893 to 1,049 m^2/g. Crystals in the size range of 2-10 μm were detected, and progressively larger particles were obtained as the H_3BTC concentration was increased. The HKUST-1 product obtained after longer reflux time and at higher ligand concentrations tends to produce larger crystals. To make a product with improved textural properties under high yield conditions, the effect of stirring speed was then investigated. Increasing the stirring speed from 150 to 300 rpm produced smaller crystals from ca. 5.0 to 3.5 μm. This formation of smaller particles is a consequence of producing a finer dispersion of substrates when higher stirring rates are applied [80]. The surface area of the HKUST-1 at 300 rpm (1,737 m^2/g) was higher than that produced at 150 rpm (1,250 m^2/g), which indicates that increasing the rate of agitation has a positive influence on the textural

quality of the HKUST-1. Even though the product yield decreased sharply at higher stirring conditions, stirring speed was still proven to be an important synthesis variable that may enable us to tune the textural properties.

Although a large number of MOF syntheses have been reported in literature, large-scale production of these materials have been neglected. Since a small scale solvothermal preparation of MOFs cannot be directly extrapolated to a commercial scale production, it is necessary to synthesize MOFs on a significantly larger scale, and most likely they have to also be formed in pellets or in tablets for industrial applications in order to be used as adsorbents or catalysts [36]. The following issues need to be taken into account for MOFs production scale-up [26]: (1) availability and cost of the starting materials, (2) synthesis conditions (low temperature, ambient pressure), (3) workup procedure, (4) activation process, (5) high product yields, (5) avoiding large amount of impurities, and (6) using only small amounts of solvents.

In 2002, the family of MOFs was extended to imidazolate-based compounds that are nowadays known as zeolitic imidazole frameworks (ZIFs) [82]. Nine imidazolate type linkers and mixtures thereof were reacted with zinc or cobalt nitrate in mixtures of DMF and DEF at various concentrations and molar ratios of metal to linker in the temperature range of 65-150 °C [83]. Among the products obtained, ZIF-8 is the most widely-investigated structure, which is Zn atoms coordinated tetrahedrally with 2-methylimidazolate (HMeIm), leading to the formula, $Zn(MeIm)_2$ [55]. ZIF-8 exhibits a *sod* topology formed by four- and six-membered ring ZnN_4 clusters with internal cavities, 1.16 nm in diameter, connected by 0.34 nm windows. ZIF-8 has been tested for gas adsorption and storage of hydrogen [84,85] and as a heterogeneous catalyst [37,86,87].

MICROWAVE-ASSISTED SYNTHESIS (SCHEME 3)

Microwave synthesis techniques have been widely applied for rapid synthesis of nanoporous materials under hydrothermal conditions [88]. Besides fast crystallization, potential advantages of this technique include phase selectivity [89,90], narrow particle size distribution [91], and facile morphology control [92,93]. Commercial microwave equipment provides adjustable power outputs and has a fiber optic temperature controller and pressure controller [81]. In microwave synthesis, a substrate mixture in a suitable solvent is transferred to a Teflon vessel, sealed and placed in the microwave
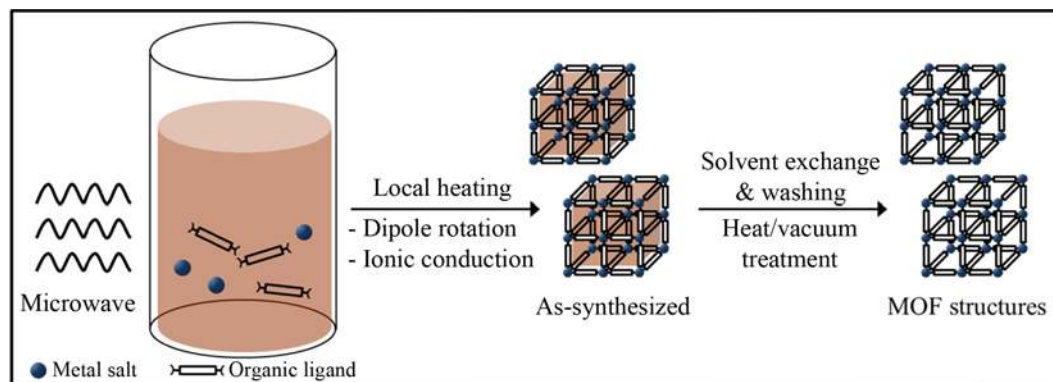
Scheme 3. Microwave-assisted solvothermal synthesis of MOF structures.

unit, and heated for the appropriate time at the set temperature. The microwave approach, where an applied oscillating electric field is coupled with the permanent dipole moment of the molecules in the synthesis medium inducing molecular rotations, results in rapid heating of the liquid phase [94,95].

The first reported microwave synthesis of MOFs was Cr-MIL-100 [62]. The compound was synthesized in 4 h at 220 °C with 44% yield, which is comparable with that of conventional hydrothermal synthesis (220 °C and 4 days). The author expanded this method to synthesis of Cr-MIL-101 at 210 °C in less than 60 min, and reported similar physicochemical and textural properties compared with the standard material synthesized using the conventional electrical heating method [96]. MOF-5 was also synthesized by applying microwave irradiation: increases in microwave irradiation time, power level, and concentration of the substrates beyond an optimal condition led to a reduction in synthesis time at the expense of crystal quality [27]. Microwave-assisted heating was found to be the method of choice to rapidly synthesize HKUST-1 crystals in the range of 10-20 μm in high yields (~90%) within 1 h [97]. Fe-MIL-53 [59], Fe-MIL-101-NH$_2$ [60], IRMOF-3 (H$_2$BDC-NH$_2$) [61], and ZIF-8 (HMeIm) [63] were also synthesized using microwave-assisted synthesis method.

Recently, systematic microwave-assisted synthesis of Co-MOF-74 reported [28], in which 0.148 mmol of cobalt nitrate hexahydrate (Co(NO$_3$)$_2$·6H$_2$O, Sigma-Aldrich) and 0.044 mmol of H$_4$DHBDC (Sigma-Aldrich) were dissolved in 18 mL of a mixed solvent (DMF : ethanol : water=1 : 1 : 1 (v/v/v)) and put into a 35 mL tube, sealed with a rubber septum and placed in a microwave oven (Discover S-class, CEM, Maximum power of 300 W). The resulting mixture was heated to 130 °C, held for 1 h, and then cooled to room temperature. The red-orange crystals were separated by centrifuging. After washing with DMF three times, they were placed in methanol, which was decanted and replenished four times for two days. The solvent was removed under vacuum at 250 °C for 5 h, yielding a dark-purple porous material. The textural properties of Co-MOF-74 samples prepared under various microwave synthesis conditions (synthesis temperature, microwave irradiation power level, and synthesis time) are summarized in Table 3. According to the results, the optimized Co-MOF-74 was synthesized at 130 °C with 180 W microwave power level for 1 h (entry 7), which resulted in the highest textural properties (1,314 m^2/g of BET surface area) with a high product yield (ca. 76% based on ligand). Co-MOF-74 (ca.

Table 3. Textural properties of Co-MOF-74 synthesized via microwave-assisted solvothermal method at different conditions [28]

| Entry | Conditions | | | S_{BET} (m^2/g)^a | V_{Pore} (cm^3/g)^b | Product yield (%) |
	Temperature (°C)	Power (W)	Time (min)			
1	100	180	60	1318	0.49	7
2	120	180	60	1319	0.51	45
3	130	120	60	1402	0.71	58
4		150	60	1411	0.69	63
5		180	30	1193	0.49	69
6		180	40	1155	0.47	75
7		180	60	1314	0.51	76
8		180	70	1273	0.51	74
9		210	30	123	0.01	84
10		210	40	1270	0.65	72
11		210	60	1321	0.50	74

^{a}S$_{BET}$=specific surface area calculated by the BET method
^{b}V$_{pore}$=total pore volume

50 μm long and 8 μm wide) by microwave heating was significantly smaller in size than Co-MOF-74 (ca. 300 μm long and 70 μm wide) solvothermally prepared.

SONOCHEMICAL SYNTHESIS (SCHEME 4)

Sonochemical methods via homogeneous and accelerated nucleation can also achieve a reduction in crystallization time and significantly smaller particles size than those by the conventional solvothermal synthesis [98,99]. As shown in Scheme 4, a substrate solution mixture for a given MOF structure is introduced to a horn-type Pyrex reactor fitted to a sonicator bar with an adjustable power output without external cooling. Formation and collapse of bubbles formed in the solution after sonication, termed acoustic cavitation, produces very high local temperatures (~5,000 K) and pressures (~1,000 bar) [99,100], and results in extremely fast heating and cooling rates (>10^{10} K/s) producing fine crystallites [26].

High-quality MOF-5 crystals in the 5-25 μm range were obtained within 30 min by sonochemical synthesis using NMP (1-methyl-2-pyrrolidone) as the solvent [29]. Detailed characterization and com-
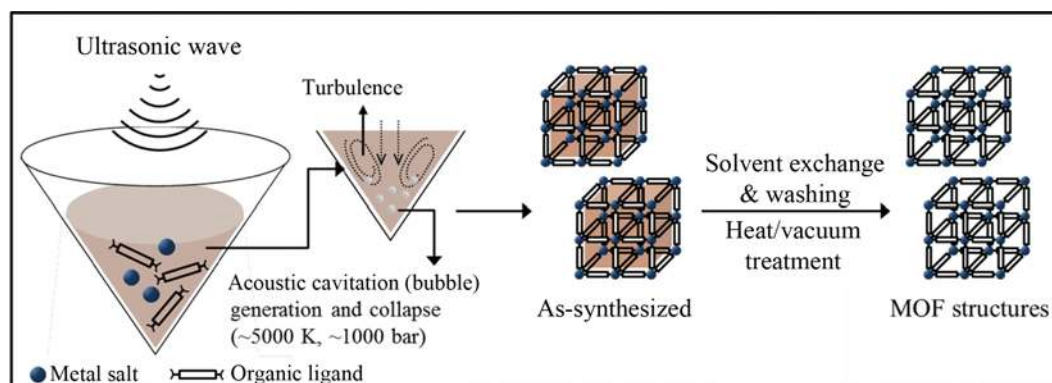
Scheme 4. Sonochemical synthesis of MOF structures.

Table 4. Textural properties of the ZIF-8 sonochemically synthesized for 1 h under different synthesis conditions[a] [37]

Entry	Batch scale (mL)	Zn^{2+} (mmol)[a]	TEA (mL)	NaOH solution (10 M, mL)	pH	S_{BET} (m^2/g)[b]	V_{pore} (cm^3/g)[c]	S_{ext} (m^2/g)[d]	Yield (%)
1[e]	50	2	-	-	6.4	1370	0.51	6.7	60
2	50	2	0.3	-	7.5	911	0.43	42.4	57
3	50	2	0.5	-	8.8	1300	0.48	13.4	59
4	50	2	0.7	-	9.2	1245	0.42	23.3	56
5	50	2	-	3.8	9.3	643	0.39	40.9	62
6	50	10	2.5	-	7.1	1197	0.60	45.3	22
7	50	10	2.5	1.0	9.3	1253	0.61	36.7	93
8	50	10	0.8	2.4	9.1	1213	0.67	79.0	96
9	50	10	0.4	3.5	9.0	1223	0.82	100.1	92
10	50	60	0.4	15.0	9.5	1249	0.71	53.7	93
11[f]	50	30	0.4	7.8	9.1	1454	0.66	15.8	60
12[g]	50	60	0.4	15.0	9.1	1226	0.51	11.7	80
13	600	720	4.5	132.0	9.2	1141	0.56	21.3	50
14[h]	600	720	4.5	132.0	9.2	1174	0.50	26.6	85
15[i]	600	720	4.5	132.0	9.2	915	0.43	12.6	84

[a]Amount of zinc salt was adjusted to keep the metal/ligand molar ratio to 2 : 2

[b]S_{BET}=specific surface area calculated by the BET method

[c]V_{pore}=total pore volume

[d]S_{ext}=external surface area calculated by the t-plot method

[e]ZIF-8 synthesized by solvothermal synthesis

[f]ZIF-8 synthesized at the condition of Zn^{2+} : MeIM=1 : 2

[g]ZIF-8 synthesized using recycled solvent with extra substrate (Zn^{2+} and MeIM) addition to maintain the molar ratio to Zn^{2+} : MeIM=2 : 2

[h]ZIF-8 synthesized in 2 h

[i]3 h

parison with a conventionally synthesized sample showed almost identical physical properties. HKUST-1 was also prepared using DMF/EtOH/H₂O mixed-solution in an ultrasonic bath [64]. The product formed after 5 min as a nanocrystalline powder (10-40 nm), and increasing the reaction time led to larger crystals (50-200 nm) and higher yields, but further reaction resulted in their partial decomposition. High-quality Mg-MOF-74 crystals (1,640 m²/g BET surface area) with particle size of ca. 0.6 μm were successfully synthesized in 1 h by a sonochemical method after triethylamine (TEA) was added as a deprotonating agent. Interestingly, mesopores were formed, probably due to the competitive binding of TEA to Mg^{2+} ions [13]. Both interpenetrated and non-interpenetrated MOF structures, i.e., PCN-6/PCN-6' and IRMOF-9/IRMOF-10, could be synthesized by simple control in ultrasonic power levels in sonochemical synthesis [31]. At lower power levels, the non-interpenetrated structures (PCN-6', IRMOF-10) were obtained, intermediate power levels led to mixtures, and higher power levels to phase-pure interpenetrated structures of the corresponding MOF (PCN-6, IRMOF-9). Uniform well-shaped particles were obtained for all the cases: 1.5-2.0 μm for PCN-6', 4.5-6.0 μm for PCN-6, and 5-20 μm for IRMOF-9 and -10.

Recently, ZIF-8 was prepared by a sonochemical method under the pH-adjusted synthesis conditions using NaOH and TEA [37]. Inexpensive industrial grade DMF was employed as a solvent. A substrate was prepared using 0.67 g (2 mmol) of zinc nitrate hexahydrate (Zn(NO₃)₂·6H₂O, 98%, Sigma-Aldrich) and 0.167 g (2 mmol) of HMeIm (98%, Sigma-Aldrich) in 50 mL of DMF (industrial grade,

DUKSAN, Korea), and stirred vigorously until a clear solution was obtained. Then, 0.3 to 0.7 mL of TEA (99%, Sigma-Aldrich) was added and the resulting solution was transferred to a 70 mL of horn-type reactor fitted to a sonicator having an adjustable power output (maximum 500 W at 20 kHz). After the synthesis, the ZIF-8 samples were washed with DMF and placed in methanol. After filtration, the samples were dried in a vacuum oven (<5×10⁻³ torr) at 80 °C. A small amount of TEA as a deprotonating agent was necessary to obtain ZIF-8 crystals when the resulting solution was subjected to an ultrasonic treatment for 1 h at a 60% power level. As summarized in Table 4, a ZIF-8 sample with the best textural properties was obtained with 0.5 mL TEA addition (entry 3). The textural properties were similar to those of ZIF-8 prepared in solvothermal method (entry 1), but sonochemically prepared ZIF-8 was ca. 700 nm in size, which was approximately 400 times smaller than ZIF-8 prepared in solvothermal method. The optimum pH for ZIF-8 synthesis was ca. 9.0 with 0.5-0.7 mL of TEA. Inferior textural properties were observed (entry 5 in Table 4) when NaOH (aq, 10 M) was tested for pH control instead of TEA, and a small amount of TEA with NaOH (aq) was used to maintain the textural properties of ZIF-8. ZIF-8 was then prepared using five-times as much synthesis substrate (entry 6, Table 4). The resulting ZIF-8 exhibited good textural properties (BET specific surface area: 1,197 m²/g, total pore volume: 0.60 cm³/g), but the product yield under these conditions was low (22%). 2.5 mL TEA was apparently not sufficient to achieve the optimum pH of 9.0 established earlier, and increasing the pH using 10 M NaOH resulted in an immediate improvement in prod-

uct yield to 93% (entry 7). Subsequently, the amount of relatively costly TEA used was decreased steadily from 2.5 to 0.8 (entry 8) and then to 0.4 mL (entry 9). No loss of yield or textural properties was observed. The amount of TEA used (HMeIM : TEA=308 : 1) is significantly less than the HMeIM : TEA=1 : 1 reported elsewhere [101]. Thirty times as much substrate was then attempted for ZIF-8 synthesis. Acceptable textural properties and 93% yield were obtained using 0.4 mL of TEA and balancing the NaOH concentration to control the pH (entry 10). The substrate ratio used in this study (Zn^{2+} : HMeIM=2 : 2) has been universally employed by most of the research groups [55,86,102]. At the Zn^{2+} : MeIM of 1 : 2 (entry 11 in Table 4), the textural properties were excellent but the product yield was unsatisfactory (60%). Synthesis using the recycled mother liquid at Zn^{2+} : MeIM=2 : 2 with addition of make-up zinc salt and ligand to keep the substrate ratio as the fresh synthesis condition (entry 12) had shown acceptable textural properties (BET specific surface area: 1,226 m^2/g, total pore volume: 0.51 cm^3/g) in good yield (80%). Finally, sonochemical synthesis was carried out on a 1 L batch scale. ZIF-8 prepared in 2 h produced good textural properties in 85% yield (entry 14). The space-time yield (STY: kilograms of product per cubic meter of reaction mixture per day, kg/m^3·day) [103] of the ZIF-8 in entry 14 was 2,140 kg/m^3·day, which was ca. 1,200 times higher than the conventional solvothermal synthesis.
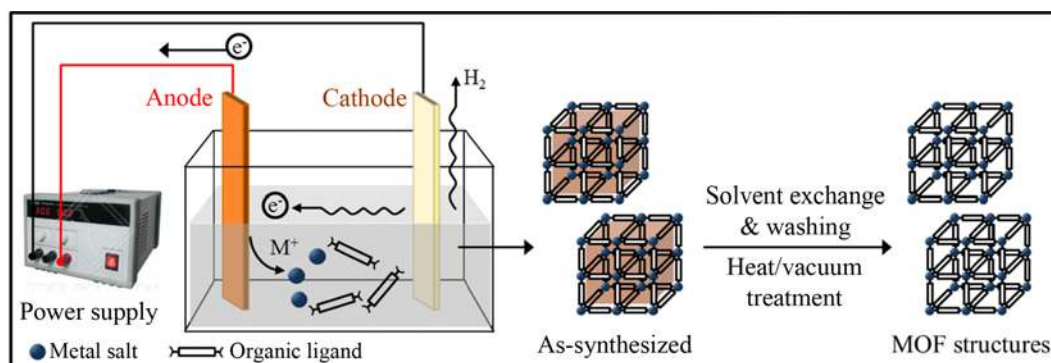
ELECTROCHEMICAL SYNTHESIS (SCHEME 5)

The electrochemical synthesis of MOFs uses metal ions contin-uously supplied through anodic dissolution as a metal source instead of metal salts, which react with the dissolved linker molecules and a conducting salt in the reaction medium. The metal deposition on the cathode is avoided by employing protic solvents, but in the process H_2 is generated [32]. The electrochemical route is also possible to run a continuous process to obtain a higher solids content compared to normal batch reactions [26].

The electrochemical synthesis of MOFs was first reported in 2005 by researchers at BASF [104] for HKUST-1. Bulk copper plates are arranged as the anodes in an electrochemical cell with the H_3BTC dissolved in methanol as solvent and a copper cathode. During a period of 150 min at a voltage of 12-19 V and a currency of 1.3 A, a greenish blue precipitate was formed. After activation, a dark blue colored powder (octahedral crystals in 0.5 to 5 μm size) having surface area of 1,820 m^2/g was obtained. This work was further extended to the ZIFs syntheses [32,105].

Recently, HKUST-1, ZIF-8, Al-MIL-100, Al-MIL-53, and Al-MIL-53-NH_2 were synthesized via anodic dissolution in an electrochemical cell [65]. The synthesis parameters such as solvent, electrolyte, voltage-current density, and temperature on the synthesis yield and textural properties of the MOFs obtained, was investigated and the produced MOF structures were characterized by X-ray diffraction, gas adsorption, atomic force microscopy, diffuse reflectance infrared Fourier transform spectroscopy, and scanning electron microscopy. For HKUST-1, the ethanol-water ratio not only affects linker solubility, but also solution conductivity and the deprotonation of the H_3BTC, and ethanol content must be above 75 vol%.

Scheme 5. Electrochemical synthesis of MOF structures.

Table 5. Textural properties of the HKUST-1 synthesized vial electrochemical method under different synthesis conditions [65]

Entry	EtOH : H_2O (v/v)	Temperature (°C)	Current (mA)	Conductivity (mS/cm)[a]	S_{BET} (m^2/g)[b]	V_{Pore} (cm^3/g)[c]
1	50 : 50	25	20	n/a	323	0.16
2	75 : 25		50	n/a	1108	0.51
3	96 : 4		100	0.53	1436	0.70
4	96 : 4	40	50	0.53	1404	0.59
5		60			1441	0.60
6		80			1355	0.62
7	96 : 4	40	50	1.86	1427	0.59
8		40	50	3.67	1553	0.69

[a]Conductivity was measured at room temperature before starting the experiments
[b]S_{BET}=specific surface area calculated by the BET method
[c]V_{pore}=total pore volume calculated at P/P_0=0.5

At low ethanol content, a different coordination polymer called cat-ena-triaqua-mu-(1,3,5-benzenetricarboxylate)-copper(II) is formed (entry 1 in Table 5). Standard synthesis solutions of 15 mmol (3.15 g) of H_3BTC with 33 mmol (1.038 g) of MTBS (tributylmethylam-monium methyl sulfate) dissolved in 100 mL 96 vol% EtOH were heated to four different temperatures in contact with two copper electrodes separated by 3 cm, and then 100 mA (entry 3 in Table 5) and 50 mA (entry 4-6 in Table 5) are passed through the system for 1 h. On average ~100 mg of dried HKUST-1 is obtained from each synthesis, and the surface areas correspond well to those given in the literature (BET area=1,400 m^2/g, pore volume=0.6 cm^3/g). No Cu_2O impurity is observed. By controlling the current density, the Cu^{2+} concentration close to the electrode can be tuned. How-ever, current density and voltage are interrelated through the sys-tem geometry and the solution conductivity. A standard synthesis solution displayed a conductivity of ca. 530 μS/cm (entry 4 in Table 5). By increasing the electrolyte concentration 5 and 15 times, con-ductivity can be increased to 1.86 and 3.6 mS/cm, respectively (entries 7 and 8). Increasing conductivity improved the yield because less energy is required to overcome the ohmic drop in the solution and can therefore be used to dissolve the electrode. As expected, higher conductivity results in higher yield. The high impact of the ohmic drop is remarkable because a 3.5 times increase in conductivity only increases the yield by a factor 1.6; and a 7 times increase in conduc-tivity only increases the yield by a factor of 2.

It was claimed that electrochemical MOF synthesis has several advantages: (1) faster synthesis at lower temperatures than conven-tional synthesis, (2) metal salts are not needed and therefore sepa-ration of anions such as NO_3^- or Cl^- from the synthesis solution is not needed prior to solvent recycle, and (3) virtual total utilization of the linker can be achieved in combination with high Faraday effi-ciencies [65]. They also found that the electrochemically synthe-sized MIL-53 sample does not exhibit the characteristic breathing effect during CO_2 adsorption at high-pressure condition [52,65].
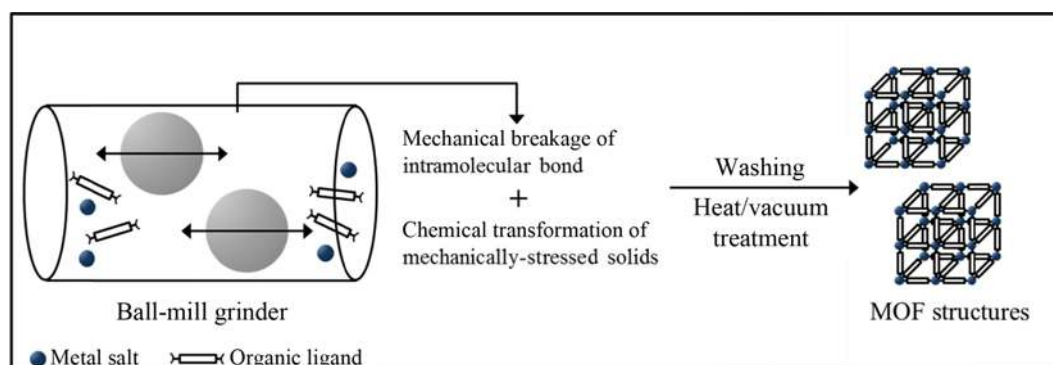
MECHANOCHEMICAL SYNTHESIS (SCHEME 6)

Mechanical breakage of intramolecular bonds followed by a chem-ical transformation takes place in mechanochemical synthesis [26]. Porous MOF synthesis by mechanochemical reaction was reported first in 2006 [106] and results of selected mechanochemical MOF synthesis studies were summarized by Friščić, recently [107]. Mech-anochemical reactions can occur at room temperature under sol-vent-free conditions, which is especially advantageous when organic solvents can be avoided [108]. Quantitative yields of small MOF particles can be obtained in short reaction times, normally in the range of 10-60 min. In many occasions, metal oxides were found to be preferred than metal salts as a starting material, which results in water as the only side product [26]. The critical contribution of moisture in mechanochemical synthesis of pillared type MOFs was recently reported by Kitagawa group [109].

The addition of small amounts of solvents in liquid-assisted grind-ing (LAG) can lead to acceleration of mechanochemical reactions due to an increase of mobility of the reactants on the molecular level [107,110]. The liquid can also work as a structure-directing agent. More recently, the extension of the method to ion- and liquid assisted grinding (ILAG) was reported to be highly efficient for the selec-tive construction of pillared-layered MOFs [34,107,111]. However, mechanochemical synthesis is limited to specific MOF types only and large amount of product is difficult to obtain.

HKUST-1 was successfully produced by mechanochemical syn-thesis method without using a solvent [66]. While a mechanochem-ical reaction between H_3BTC and copper acetate produces HKUST-1, reaction using copper formate resulted in a previously unknown phase, potentially due to templating effects of the different acid by-products formed [66]. The solventless produced HKUST-1 showed 1,084 m^2/g of BET surface area. LAG after 100 μL of MeOH addi-tion, the BET surface area increased to 1,364 m^2/g with slightly sharper XRPD patterns [66]. Recently, a mechanochemical approach was also applied for ZIF synthesis using combinations of ZnO and imida-zole (HIm), 2-methylimidazole (HMeIm), and 2-ethylimidazole (HEtIm) as the starting material within 30-60 min reaction time [67]. Table 6 summarizes the outcome of the investigation. The ILAG was found to accelerate the formation and direct the phase formed, and the synthesis of ZIFs was facilitated in the presence of the am-monium ions. ZIF-8 was successfully synthesized in a combination of ZnO and HMeIm within 30 min in the presence of NH_4NO_3 using DEF as a solvent and ZIF-4 was also successfully synthesized in a combination of ZnO and HIm within 30 min in the presence of NH_4 NCH_3SO_3 using DMF as a solvent. Interestingly, for a reaction using a combination of ZnO and HEtIm in the presence of NH_4NO_3, *rho* topologies were obtained after 5-10 min. However, the *rho* topologies were changed after 20 min grinding to *ana* topologies, and finally nonporous *qtz* framework. But with DEF as the grinding liquid, the

Scheme 6. Mechanochemical synthesis of MOF structures.

Table 6. ZIF topologies obtained in mechanochemical screening[a] [67]

Ligand	Liquid	Salt			
		None	NH$_4$NO$_3$	NH$_4$MeSO$_3$	(NH$_4$)$_2$SO$_4$
HIm	none	mixture[b]	zni[c]	zni[c]	mixture
HIm	DMF	cag	cag	cag	cag
HIm	DEF	-[d]	nog	unknown[e]	unknown
HIm	EtOH	zni	zni	zni	zni
HMeIm	none	-	sod	sod	-
HMeIm	DMF	sod	sod	sod	sod
HMeIm	DEF	sod	sod	sod	sod
HMeIm	EtOH	sod	sod	sod	sod
HEtIm	none	-	qtz	rho[f]	-
HEtIm	DMF	-	qtz	ana	rho
HEtIm	DEF	-	qtz	ana	rho
HEtIm	EtOH	-	qtz	qtz	rho

[a]Each product was obtained by grinding for 30 min
[b]Mixture of starting materials
[c]zni-type ZIF and an as yet unidentified material characterized by reflections in the 2θ range 10-20°
[d]No reaction is evident initially, but 24 h aging leads to cag- or nog-type ZIFs
[e]Initial product is an as yet unidentified material, characterized by a reflection at 5.6°, which transforms into the nog-type ZIF on 24 h aging
[f]Forms the qtz-type ZIF on 7 days aging

ana topology was the only product even after 60 min grinding, and with (NH$_4$)$_2$SO$_4$ as the salt additive the rho topology remained the only product even after 60 min.

OTHERS

1. Ionic Liquids (ILs) as a Synthesis Medium

As described above, MOFs are typically synthesized in organic solvents or in water, but have also been prepared in ionic liquids (ILs) recently (Scheme 7) [112,113]. ILs have been attracting attention as a solvent for chemical synthesis, because of their unique properties such as essentially zero vapor pressure, excellent solvating properties, easy recyclability, and high thermal stability. [114,115] The majority of the reports dealing with MOF synthesis have focused on ILs derived from 1-alkyl-3-methylimidazolium; however, deep eutectic solvents (DESs), mixtures of two or more compounds that have melting points lower than that of either of their constituents, are also known to exhibit solvent properties very similar to those of ILs [116] and have been employed for MOF synthesis [115]. They have advantages over other types of ILs such as ease of preparation as pure phases from easily available components, low prices, and relative unreactivity towards atmospheric moisture [114]. Very recently, HKUST-1 was prepared in sonochemical synthesis using choline chloride/dimethylurea DES as a solvent [114]. Effects of various synthesis parameters on the crystallization process of HKUST-1 were examined, and the properties of the sample were compared to those of HKUST-1 prepared via a conventional ionothermal synthesis route in an oven.

### 2. Microfluidic MOF Synthesis System

The development of continuous, faster and viable processes for MOF synthesis would be desirable to meet commercial and industrial requirements [117], and microfluidic synthesis of MOFs can be considered for this purpose (Scheme 8). Recently, preparation of HKUST-1 was investigated using a microfluidic device [118,119]. Initially, two kinds of substrate mixtures were prepared; the aqueous phase was prepared by adding Cu(OAc)$_2$·H$_2$O and polyvinylalcohol in water (CuO particles formed were removed by centrifuging after 30 min stirring) at room temperature, whereas the organic ligand solution was prepared by dissolving H$_3$BTC in 1-octanol and heated to 60 °C. Both immiscible liquids are supplied by syringe pumps to a T-junction, where the formation of aqueous solution droplets in the continuous organic phase takes place. The HKUST-1 capsule shell is formed at the liquid-liquid interface while these droplets travel through hydrophobic polytetrafluoroethylene tubing, before collection in ethanol. The remaining 1-octanol was removed by repeatedly exchanging the supernatant with fresh ethanol. The resulting HKUST-1 capsule walls were approximately 4 mm thick, and had a macroporous structure outside, but the inner layer of the shell still consisted of densely packed crystallites [118].
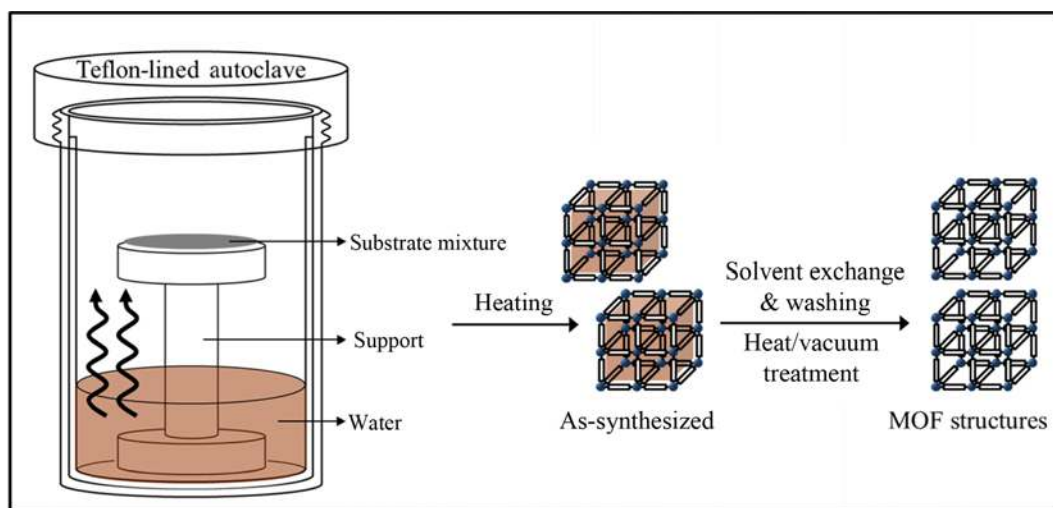
3. Dry-gel Conversion MOF Synthesis

Dry-gel conversion (DGC) synthesis method has been applied widely to the preparation of zeolites and zeolite membranes [120, 121], in which a dry amorphous aluminosilicate gel is transformed to crystalline zeolite upon contact with the vapors of water and volatile amines. The DGC method was further classified into two separate methods: (i) the vapor-phase transport (VPT) method in which a
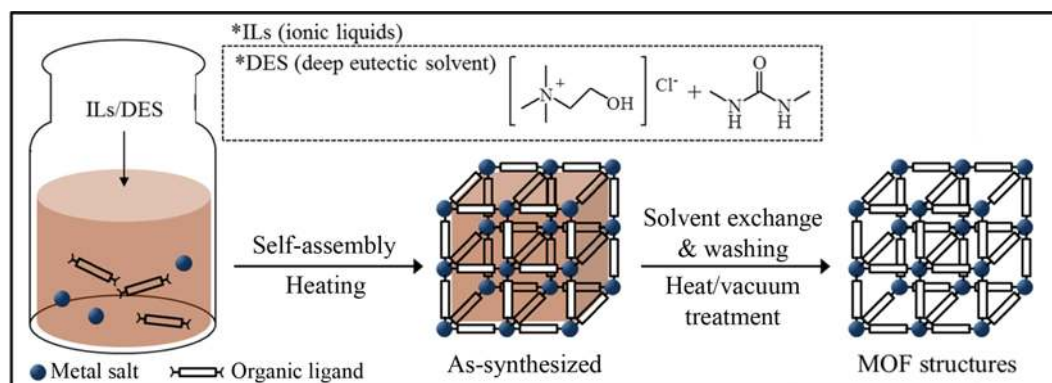
Scheme 7. Ionothermal synthesis of MOF structures.
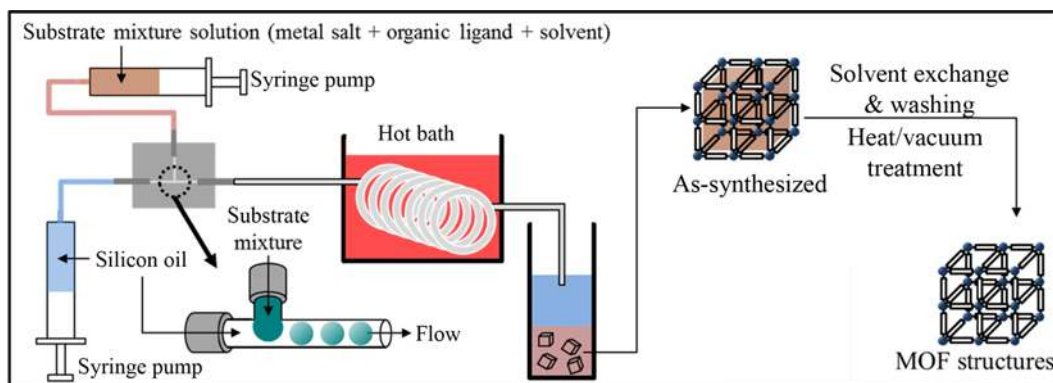
Scheme 8. Microfluidics synthesis of MOF structures.

Scheme 9. Dry-gel conversion synthesis of MOF structures.

dry gel is crystallized in the vapor of water and volatile amine, and (ii) the steam-assisted crystallization (SAC) method in which a dry-gel containing a non-volatile amine is crystallized in the steam [122]. An obvious advantage of the DGC method lies in minimization of waste disposal, reduction of reaction volume, and complete conversion of gel to uniform crystalline zeolites with a high yield. Recently, ZIF-8 [123] and Fe-MIL-100 [124] were prepared by DGC synthesis method as an environmentally benign route (Scheme 9). The water steam penetrates into the surface of eutectic mixtures of substrate (Zn(OAc)$_2$·2H$_2$O and HmIM) and excess amount of HmIM, and the condensed composites dynamically rearrange to a ZIF-8 after reaction at 120 °C for 24 h [123]. Fe-MIL-100 was obtained rapidly using metallic iron (Fe^0) and H$_3$BTC from DGC method at 165 °C for 4 days without any acid and salt addition [124].

CONCLUDING REMARKS

MOFs are currently receiving explosive attention due to their exceptional textural properties and diverse post-synthesis organic modifications feasible. For these MOFs synthesis, scale-up in solvothermal/hydrothermal synthesis as well as attempts on alternative synthesis methods need further optimization. This review presented a short summary to the currently available MOFs synthesis meth-

ods with the scope limited to several key MOF structures that can be important to chemical engineers and can be easily extended to other structures. MOF-5, HKUST-1, MIL-101, and ZIF-8 are those that can be synthesized with common organic ligands of commercial terephthalic acid (1,4-benzenedicarboxylic acid), 1,3,5-benzenetricarboxylic acid, and 2-methylimidazole in conjunction with metal nodes of Zn^{2+}, Cu^{2+}, and Cr^{3+}. Starting from the conventional solvothermal/hydrothermal synthesis, microwave-assisted, sonochemical, electrochemical, mechanochemical, ionothermal, dry-gel conversion, and microfluidic synthesis methods were discussed with specific examples. From this mini review, the following conclusions can be drawn for engineering applications of MOFs:

(1) Virtually unlimited MOFs with different structures and chemical compositions are possible, but synthesis of those with high hydrothermal stability should be considered preferentially for industrial implementation.

(2) MOFs synthesis reported is mostly confined to very small scale just sufficient for crystal structure analysis, and often not optimized. Reliable recipes for synthesis of reasonable amount of MOF material are highly desirable, much as those available for zeolites and mesoporous silicas.

(3) Textural properties reported for some MOFs such as Cr-MIL-101 are widely different, depending on the research groups. Repro-

ducible synthesis with purification details should be established.

(4) More synthesis scale-up studies for MOFs should be conducted for optimized and economic MOF materials for their industrial implementation as adsorbent, catalyst, and as a template for advanced materials. Cheap organic ligands and industrial grade solvents need to be utilized for synthesis. Low temperature/pressure conditions and high product yields are desirable. MOFs usually demands for solvent exchange and high vacuum for activation, which should be changed to a more moderate activation processes.

(5) Shaping process of converting MOF powders to pellets or monolith need further investigation. Some loss of original advantage in textural properties may take place in the process.

(6) MOFs were prepared by diffusion synthesis methods at room temperature and now mostly prepared by solvothermal/hydrothermal routes. These can be further supplemented by newly-attempted ionothermal synthesis, continuous microfluidic synthesis, dry-gel conversion synthesis or mechanochemical method, which can lead to more environmentally benign MOF products.

(7) MOF synthesis can be expanded to the synthesis of combined forms with other organic inorganic materials such as core-shell structures and composites.

ACKNOWLEDGEMENT

REFERENCES

1. J. R. Long and O. M. Yaghi, *Chem. Soc. Rev.*, **38**, 1213 (2009).
2. M. Eddaoudi, D. B. Moler and H. Li, *Acc. Chem. Res.*, **34**, 319 (2001).
3. D. J. Tranchemontagne, J. L. Mendoza-Cortes, M. O'Keeffe and O. M. Yaghi, *Chem. Soc. Rev.*, **38**, 1257 (2009).
4. J. R. Li, R. J. Kuppler and H. C. Zhou, *Chem. Soc. Rev.*, **38**, 1477 (2009).
5. A. U. Czaja, N. Trukhan and U. Müller, *Chem. Soc. Rev.*, **38**, 1284 (2009).
6. R. E. Morris and P. S. Wheatley, *Angew. Chem. Int. Ed.*, **47**, 4966 (2008).
7. Y. H. Hu and L. Zhang, *Adv. Mater.*, **22**, E117 (2010).
8. D. Zhao, D. Q. Yuan, D. F. Sun and H. C. Zhou, *J. Am. Chem. Soc.*, **131**, 9186 (2009).
9. D. Yuan, D. Zhao, D. Sun and H. C. Zhou, *Angew. Chem., Int. Ed.*, **49**, 5357 (2010).
10. J. L. C. Rowsell, E. C. Spencer, J. Eckert, J. A. K. Howard and O. M. Yaghi, *Science*, **309**, 1350 (2005).
11. G. Férey, M. Latroche, C. Serre, F. Millange, T. Loiseau and A. P. Guégan, *Chem. Commun.*, 2976 (2003).
12. R. Kitaura, K. Seki, G. Akiyama and S. Kitagawa, *Angew. Chem. Int. Ed.*, **42**, 428 (2003).
13. D. A. Yang, H. Y. Cho, J. Kim, S. T. Yang and W. S. Ahn, *Energy Environ. Sci.*, **5**, 6465 (2012).
14. E. Haque, J. E. Lee, I. T. Jang, Y. K. Hwang, J. S. Chang, J. Jegal and S. H. Jhung, *J. Hazard. Mater.*, **181**, 535 (2010).
15. E. Haque, J. W. Jun and S. H. Jhung, *J. Hazard. Mater.*, **185**, 507

16. S. H. Jhung, J. H. Lee, J. W. Yoon, C. Serre, G. Férey and J. S. Chang, *Adv. Mater.*, **19**, 121 (2007).
17. S. Bhattacharjee, D. A. Yang and W. S. Ahn, *Chem. Commun.*, **47**, 3637 (2011).
18. J. Kim, S. N. Kim, H. G. Jang, G. Seo and W. S. Ahn, *Appl. Catal. A: Gen.*, **453**, 175 (2013).
19. J. Y. Lee, O. K. Farha, J. Roberts, K. A. Scheidt, S. T. Nguyen and J. T. Hupp, *Chem. Soc. Rev.*, **38**, 1450 (2009).
20. S. Achmann, G. Hagen, J. Kita, I. M. Malkowsky, C. Kiener and R. Moos, *Sensors*, **9**, 1574 (2009).
21. S. M. Humphrey and P. T. Wood, *J. Am. Chem. Soc.*, **126**, 13236 (2004).
22. P. Horcajada, T. Chalati, C. Serre, B. Gillet, C. Sebrie, T. Baati, J. F. Eubank, D. Heurtaux, P. Clayette, C. Kreuz, J. S. Chang, Y. K. Hwang, V. Marsaud, P. Bories, L. Cynober, S. Gil, G. Férey, P. Couvreur and R. Gref, *Nat. Mater.*, **9**, 172 (2010).
23. N. A. Khan, Md. M. Haque and S. H. Jhung, *Eur. J. Inorg. Chem.*, 4975 (2010).
24. J. Rocha, L. D. Carlos, F. A. A. Paz and D. Ananias, *Chem. Soc. Rev.*, **40**, 926 (2011).
25. S. H. Jhung, N. A. Khan and Z. Hasan, *CrystEngComm.*, **14**, 7099 (2012).
26. N. Stock and S. Biswas, *Chem. Rev.*, **112**, 933 (2012).
27. J. S. Choi, W. J. Son, J. Kim and W. S. Ahn, *Micropor. Mesopor. Mater.*, **116**, 727 (2008).
28. H. Y. Cho, D. A. Yang, J. Kim, S. Y. Jeong and W. S. Ahn, *Catal. Today*, **185**, 35 (2012) .
29. W. J. Son, J. Kim, J. Kim and W. S. Ahn, *Chem. Commun.*, 6336 (2008).
30. D. W. Jung, D. A. Yang, J. Kim, J. Kim and W. S. Ahn, *Dalton Trans.*, **39**, 2883 (2010).
31. J. Kim, S. T. Yang, S. B. Choi, J. Sim, J. Kim and W. S. Ahn, *J. Mater. Chem.*, **21**, 3070 (2011).
32. U. Mueller, M. Schubert, F. Teich, H. Puetter, K. Schierle-Arndt and J. Pastre, *J. Mater. Chem.*, **16**, 626 (2006).
33. M. Hartmann, S. Kunz, D. Himsl, O. Tangermann, S. Ernst and A. Wagener, *Langmuir*, **24**, 8634 (2008).
34. T. Friščić, D. G. Reid, I. Halasz, R. S. Stein, R. E. Dinnebier and M. J. Duer, *Angew. Chem. Int. Ed.*, **49**, 712 (2010).
35. M. Klimakow, P. Klobes, A. F. Thüunemann, K. Rademann and F. Emmerling, *Chem. Mater.*, **22**, 5216 (2010).
36. J. Kim, S. H. Kim, S. T. Yang and W. S. Ahn, *Micropor. Mesopor. Mater.*, **161**, 48 (2012).
37. H. Y. Cho, J. Kim, S. N. Kim and W. S. Ahn, *Micropor. Mesopor. Mater.*, **169**, 180 (2013).
38. H. Li, M. Eddaoudi, M. O'Keeffe and O. M. Yaghi, *Nature*, **402**, 276 (1999).
39. A. R. Millward and O. M. Yaghi, *J. Am. Chem. Soc.*, **127**, 17998 (2005).
40. N. T. S. Phan, K. K. A. Le and T. D. Phan, *Appl. Catal. A: Gen.*, **382**, 246 (2010).
41. S. S.-Y. Chui, S. M.-F. Lo, J. P. H. Charmant, A. G. Orpen and I. D. Williams, *Science*, **283**, 1148 (1999).
42. G. Férey, C. M. Drazniekes, C. Serre, F. Millange, J. Dutour, S. Surblé and I. Margiolaki, *Science*, **309**, 2040 (2005).
43. Y. K. Hwang, D. Y. Hong, J. S. Chang, S. H. Jhung, Y. K. Seo, J.

Kim, A. Vimony, M. Daturi, C. Serre and G. Férey, *Angew. Chem. Int. Ed.*, **47**, 4144 (2008).

44. J. Kim, S. Bhattacharjee, K. E. Jeong, S. Y. Jeong and W. S. Ahn, *Chem. Commun.*, 3904 (2009).

45. P. Horcajada, C. Serre, M. V. Regí, M. Sebban, F. Taulelle and G. Férey, *Angew. Chem. Int. Ed.*, **45**, 5974 (2006).

46. A. Henschel, K. Gedrich, R. Kraehnertb and S. Kaskel, *Chem. Commun.*, 4192 (2008).

47. J. Gascon, U. Aktay, M. D. Hernandez-Alonso, G. P. M. van Klink and F. Kapteijn, *J. Catal.*, **261**, 75 (2009).

48. D. Britt, H. Furukawa, B. Wang, T. G. Glover and O. M. Yaghi, *PNAS*, **106**, 20637 (2009).

49. S. R. Caskey, A. G. Wong-Foy and A. J. Matzger, *J. Am. Chem. Soc.*, **130**, 10870 (2008).

50. C. Serre, F. Millange, C. Thouvenot, M. Nogués, G. Marsolier, D. Louër and G. Férey, *J. Am. Chem. Soc.*, **124**, 13519 (2002).

51. S. Couck, J. F. M. Denayer, G. V. Baron, T. Rémy, J. Gascon and F. Kapteijn, *J. Am. Chem. Soc.*, **131**, 6326 (2009).

52. J. Kim, W. Y. Kim and W. S. Ahn, *Fuel*, **102**, 574 (2012).

53. P. Horcajada, S. Surblé, C. Serre, D. Y. Hong, Y. K. Seo, J. S. Chang, J. M. Grenèche, I. Margiolaki and G. Férey, *Chem. Commun.*, 2820 (2007).

54. M. Kim and S. M. Cohen, *CrystEngComm.*, **14**, 4096 (2012).

55. K. S. Park, Z. Ni, A. P. Côté, J. Y. Choi, R. Huang, F. J. Uribe-Romo, H. K. Chae, M. O'Keeffe and O. M. Yaghi, *PNAS*, **103**, 10186 (2006).

56. R. Banerjee, A. Phan, B. Wang, C. Knobler, H. Furukawa, M. O'Keeffe and O. M. Yaghi, *Science*, **319**, 939 (2008).

57. M. Eddaoudi, J. Kim, N. Rosi, D. Vodak, J. Wachter, M. O'Keeffe and O. M. Yaghi, *Science*, **295**, 469 (2002).

58. H. R. Abid, H. Tian, H. M. Ang, M. O. Tade, C. E. Buckley and S. Wang, *Chem. Eng. J.*, **187**, 415 (2012).

59. K. M. L. Taylor-Pashow, J. D. Rocca, Z. Xie, S. Tran and W. Lin, *J. Am. Chem. Soc.*, **131**, 14261 (2009).

60. Z. Ni and R. I. Masel, *J. Am. Chem. Soc.*, **128**, 12394 (2006).

61. Y. K. Seo, G. Hundal, I. T. Jang, Y. K. Hwang, C. H. Jun and J. S. Chang, *Micropor. Mesopor. Mater.*, **119**, 331 (2009).

62. S. H. Jhung, J. H. Lee and J. S. Chang, *Bull. Korean Chem. Soc.*, **26**, 880 (2005).

63. J. H. Park, S. H. Park and S. H. Jhung, *J. Korean Chem. Soc.*, **53**, 553 (2009).

64. Z. Q. Li, L. G. Qiu, T. Su, Y. Wu, W. Wang, Z. Y. Wu and X. Jiang, *Mater. Lett.*, **63**, 78 (2009).

65. A. M. Joaristi, J. Juan-AlcanÞiz, P. Serra-Crespo, F. Kapteijn and J. Gascon, *Cryst. Growth Des.*, **12**, 3489 (2012).

66. A. Pichon and S. L. James, *CrystEngComm.*, **10**, 1839 (2008).

67. P. J. Beldon, L. Fábián, R. S. Stein, A. Thirumurugan, A. K. Cheetham and T. Friščić, *Angew. Chem. Int. Ed.*, **49**, 9640 (2010).

68. N. Stock, *Micropor. Mesopor. Mater.*, **129**, 287 (2010).

69. D. Kim, T. B. Lee, S. B. Choi, J. H. Yoon, J. Kim and S. H. Choi, *Chem. Phys. Lett.*, **420**, 256 (2006).

70. D. J. Tranchemontagne, J. R. Hunt and O. M. Yaghi, *Tetrahedron*, **64**, 8553 (2008).

71. D. Y. Hong, Y. K. Hwang, C. Serre, G. Férey and J. S. Chang, *Adv. Funct. Mater.*, **19**, 1537 (2009).

72. Y. Pan, B. Yuan, Y. Li and D. He, *Chem. Commun.*, **46**, 2280 (2010).

73. J. Yang, Q. Zhao, J. Li and J. Dong, *Micropor. Mesopor. Mater.*, **130**, 174 (2010).

74. N. A. Khan, I. J. Kang, H. Y. Seok and S. H. Jhung, *Chem. Eng. J.*, **166**, 1152 (2011).

75. T. Loiseau, C. Serre, C. Huguenard, G. Fink, F. Taulelle, M. Henry, T. Bataille and G. Férey, *Chem. Eur. J.*, **10**, 1373 (2004).

76. N. A. Ramsahye, G. Maurin, S. Bourrelly, P. Llewellyn, T. Loiseau and G. Férey, *Phys. Chem. Chem. Phys.*, **9**, 1059 (2007).

77. M. Kandiah, M. H. Nilsen, S. Usseglio, S. Jakobsen, U. Olsbye, M. Tilset, C. Larabi, E. A. Quadrelli, F. Bonino and K. P. Lillerud, *Chem. Mater.*, **22**, 6632 (2010).

78. Q. M. Wang, D. Shen, M. Bulow, M. L. Lau, S. Deng, F. R. Fitch, N. O. Lemcoff and J. Semanscin, *Micropor. Mesopor. Mater.*, **55**, 217 (2002).

79. K. Schlichte, T. Kratzke and S. Kaskel, *Micropor. Mesopor. Mater.*, **73**, 81 (2004).

80. T. Mateovic, B. Kriznar, M. Bogataj and A. Mrhar, *J. Microencapsulation*, **19**, 29 (2002).

81. J. Kim, H. Y. Cho and W. S. Ahn, *Catal. Survey Asia*, **16**, 106 (2012).

82. Y. Q. Tian, C. X. Cai, Y. Ji, X. Z. You, S. M. Peng and G. H. Lee, *Angew. Chem., Int. Ed.*, **41**, 1384 (2002).

83. R. Banerjee, A. Phan, B. Wang, C. Knobler, H. Furukawa, M. O'Keeffe and O. M. Yaghi, *Science*, **319**, 939 (2008).

84. H. Wu, W. Zhou and T. Yildirim, *J. Am. Chem. Soc.*, **129**, 5314 (2007).

85. B. Assfour, S. Leoni and G. Seifer, *J. Phys. Chem. C*, **114**, 13381 (2010).

86. U. P. N. Tran, K. K. A. Le and N. T. S. Phan, *ACS Catal.*, **1**, 120 (2011).

87. C. M. Miralda, E. E. Macias, M. Zhu, P. Ratnasamy and M. A. Carreon, *ACS Catal.*, **2** 180 (2012).

88. S. E. Park, J. S. Chang, Y. K. Hwang, D. S. Kim, S. H. Jhung and J. S. Hwang, *Catal. Survey Asia*, **8**, 91 (2004).

89. S. H. Jhung, J. S. Chang, J. S. Hwang and S. E. Park, *Micropor. Mesopor. Mater.*, **64**, 33 (2003).

90. S. H. Jhung, J. H. Lee, J. W. Yoon, J. S. Hwang, S. E. Park and J. S. Chang, *Micropor. Mesopor. Mater.*, **80**, 147 (2005).

91. K. K. Kang, C. H. Park and W. S. Ahn, *Catal. Lett.*, **59**, 45 (1999).

92. S. H. Jhung, J. S. Chang, Y. K. Hwang and S. E. Park, *J. Mater. Chem.*, **14**, 280 (2004).

93. Y. K. Hwang, J. S. Chang, S. E. Park, D. S. Kim, Y. U. Kwon, S. H. Jhung, J. S. Hwang and M. S. Park, *Angew. Chem. Int. Ed.*, **44**, 557 (2005).

94. R. Kerner, O. Palchik and A. Gedanken, *Chem. Mater.*, **13**, 1413 (2001).

95. Y. P. Xu, Z. J. Tian, S. J. Wang, Y. Hu, L. Wang, B. C. Wang, Y. C. Ma, L. Hou, J. Y. Yu and L. W. Lin, *Angew. Chem. Int. Ed.*, **45**, 3965 (2006).

96. S. H. Jhung, J. H. Lee, J. W. Yoon, C. Serre, G. Férey and J. S. Chang, *Adv. Mater.*, **19**, 121 (2007).

97. M. Schlesinger, S. Schulze, M. Hietschold and M. Mehring, *Micropor. Mesopor. Mater.*, **132**, 121 (2010).

98. K. S. Suslick, S. B. Choe, A. A. Cichowlas and M. W. Grinstaff, *Nature*, **353**, 414 (1991).

99. A. Gedanken, *Ultrason. Sonochem.*, **11**, 47 (2004).

100. K. S. Suslick, D. A. Hammerton and R. E. Cline, *J. Am. Chem. Soc.*, **108**, 5641 (1986).

101. A. F. Gross, E. Sherman and J. J. Vajo, *Dalton Trans.*, **41**, 5458

(2012).

102. Z. Zhang, S. Xian, H. Xi, H. Wang and Z. Li, *Chem. Eng. Sci.*, **66**, 4878 (2011).

103. D. Farrusseng, *Metal-Organic Frameworks-Applications from Catalysis to Gas Storage*, Wiley VCH Verlag GmbH & Co. KGaA, Weinheim (2011).

104. U. Mueller, H. Puetter, M. Hesse and H. Wessel, PCT Patent, 049,892 (2005).

105. I. Richter, M. Schubert and U. Müller, PCT Patent, 131,955 (2007).

106. A. Pichon, A. Lazuen-Garay and S. L. James, *CrystEngComm.*, **8**, 211 (2006).

107. T. Friščić, *J. Mater. Chem.*, **20**, 7599 (2010).

108. A. Lazuen-Garay, A. Pichon and S. L. James, *Chem. Soc. Rev.*, **36**, 846 (2007).

109. H. Sakamoto, R. Matsuda and S. Kitagawa, *Dalton Trans.*, **41**, 3956 (2012).

110. T. Friščić, and L. Fábián, *CrystEngComm.*, **11**, 743 (2009).

111. P. J. Beldon, L. Fábián, R. S. Stein, A. Thirumurugan, A. K. Cheetham and T. Friščić, *Angew. Chem. Int. Ed.*, **49**, 9640 (2010).

112. L. Liu, H. Wei, L. Zhang, J. Li and J. Dong, *Stud. Surf. Sci. Catal.*, **174**, 459 (2008).

113. F. Himeur, I. Stein, D. S. Wragg, A. M. Z. Slawin, P. Lightfoot and R. E. Morris, *Solid State Sci.*, **12**, 418 (2010).

114. S. H. Kim, S. T. Yang, J. Kim and W. S. Ahn, *Bull. Korean Chem. Soc.*, **32**, 2783 (2011).

115. J. Zhang, T. Wu, S. Chen, P. Feng and X. Bu, *Angew. Chem. Int. Ed.*, **48**, 3486 (2009).

116. Z. Lin, A. M. Z. Slawin and R. E. Morris, *J. Am. Chem. Soc.*, **129**, 4880 (2007).

117. P. M. Schoenecker, G. A. Belancik, B. E. Grabicka and K. S. Walton, *AIChE J.*, **59**, 1255 (2013).

118. R. Ameloot, F. Vermoortele, W. Vanhove, M. B. J. Roeffaers, B. F. Sels and D. E. De Vos, *Nature Chem.*, **3**, 382 (2011).

119. D. Witters, N. Vergauwe, R. Ameloot, S. Vermeir, D. De Vos, R. Puers, B. Sels and J. Lammertyn, *Adv. Mater.*, **24**, 1316 (2012).

120. W. Xu, J. Dong, J. Li and F. Wu, *J. Chem. Soc. Chem. Commun.*, 755 (1990).

121. A. J. J. Koekkoek, V. Degirmenci and E. J. M. Hensen, *J. Mater. Chem.*, **21**, 9279 (2011).

122. M. Matsukata, M. Ogura, T. Osaki, P. R. H. P. Rao, M. Nomura and E. Kikuchi, *Topics in Catal.*, **9**, 77 (1999).

123. Q. Shi, Z. Chen, Z. Song, J. Li and J. Dong, *Angew. Chem. Int. Ed.*, **50**, 672 (2011).

124. I. Ahmed, J. Jeon, N. A. Khan and S. H. Jhung, *Cryst. Growth Des.*, **12**, 5878 (2012).